The WSRT HALOGAS Survey:
HI Observations and Models of NGC 4244

Laura K. Zschaechner, Richard J. Rand, George H. Heald,
Gianfranco Gentile, Peter Kamphuis and the HALOGAS Team

Hydrogen Accretion in LOcal GAlaxieS

Introduction

There exists a correlation between the presence of extra-planar radio continuum, diffuse ionized gas (DIG), X-ray, and dust with galaxy disk star formation (e. g. Rossa & Dettmar 2003, Tullmann et al. 2006A, Howk & Savage 1999). This favors disk-halo flows as likely origins for these components. However, no such correlation has been established for HI. This may suggest more than one origin for extra-planar HI but may also be partly due to the lack of a systematic survey. HALOGAS is such a survey.

A clue to halo origins lies in their kinematics. Trends concerning extra-planar HI, such as the presence and magnitude of any decreases in rotation speed with height (lags) or correlations with the kinematics of DIG layers are useful in determining its origins. Furthermore, any radial variations of lags also yield insight. Recent measurements show lags in multiple DIG layers (Heald et al. 2007), leading to models which attempt to understand this gradient in terms of disk-halo flows and accretion of primordial gas.

NGC 4244, which has a star formation rate of 0.12 $M_{\odot}$ yr^{-1}, is on the low star-forming end of the HALOGAS sample. NGC 4244 is highly inclined, which also allows an accurate estimate for the lag. For these reasons it will provide substantial insight concerning any connection between star formation and HI halo properties.

Figure 3. bv plots showing each category of model attempted with no lag. Crosses indicate an exceptionally poor fit, blank a somewhat poor fit, boxes a reasonable fit and asterisks a good fit. These are judged through visual inspection. The favored models are surrounded with orange boxes.

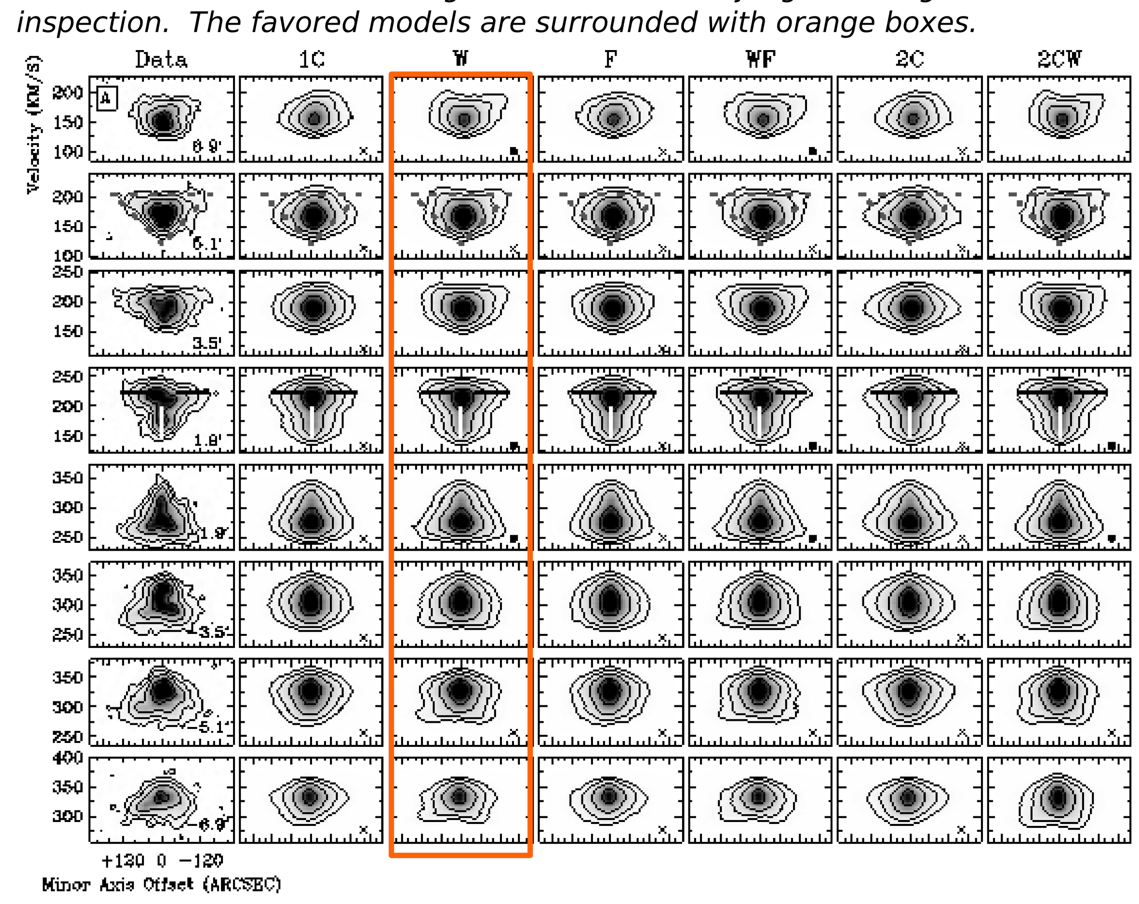

Contours: 0.18x3ⁿ mJy/beam

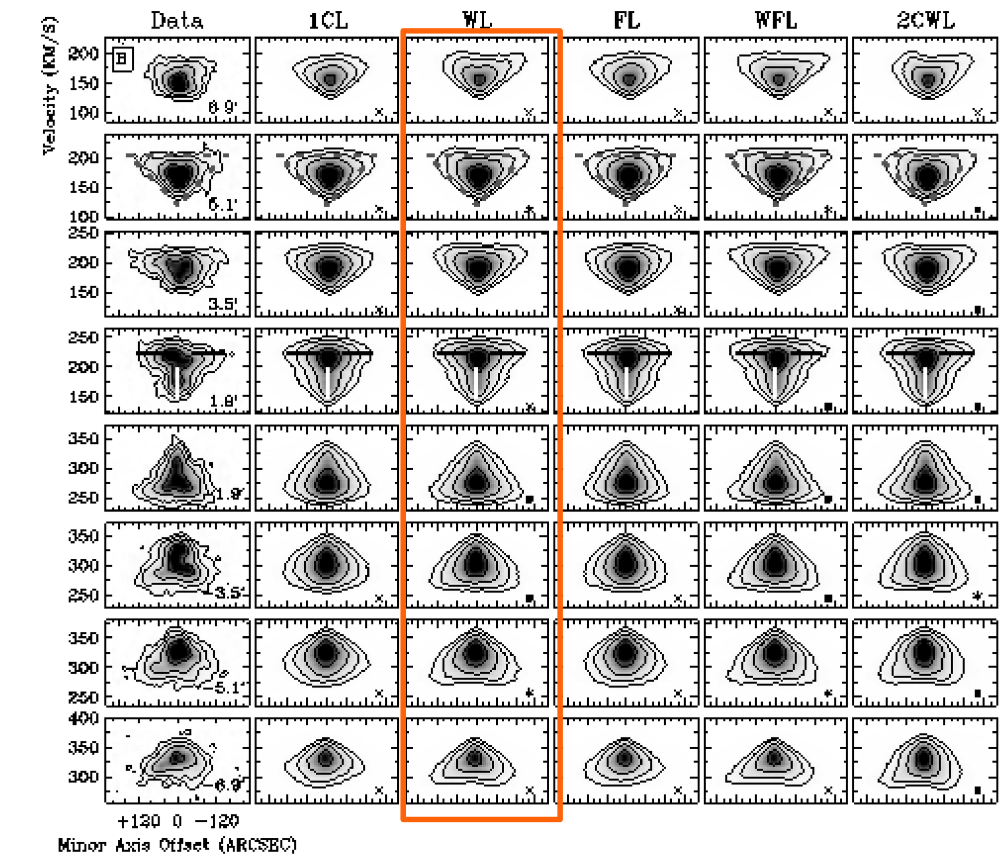

Figure 4. Analogous to plots shown in Figure 3, but with the addition of lags as well as the omission of the 2C model. The magnitudes of lags in km s^{-1} kpc^{-1} are -7 for 1CL as well as FL, and -9 for WL, WFL, and 2CWL.

Observations and Data

Details concerning the observations may be found on the HALOGAS website: http://www.astron.nl/halogas/

For NGC 4244, We use a 21x13.5" cube with a position angle of -0.69°. Also, a 30x30" cube is examined for fainter emission. The velocity resolution of each cube is 4.12 km/s.

Figures 1 and 2 provide a partial representation of the data. Properties to note are the minor asymmetries, evidence for a thickened disk, and a warp component perpendicular to the line of sight.

Figure 1. (below, left)
Zeroth-Moment map of NGC 4244. The 21x13.5" beam is shown in the lower left-hand corner. Diagonal solid lines represent slice locations for the bv diagrams in Figures 3 and 4 and the dashed lines show the radial extent of slices in Figure 5. The northern half is approaching, while the southern receding. Note the warp component perpendicular to the line of sight and radially tapered outer edges.

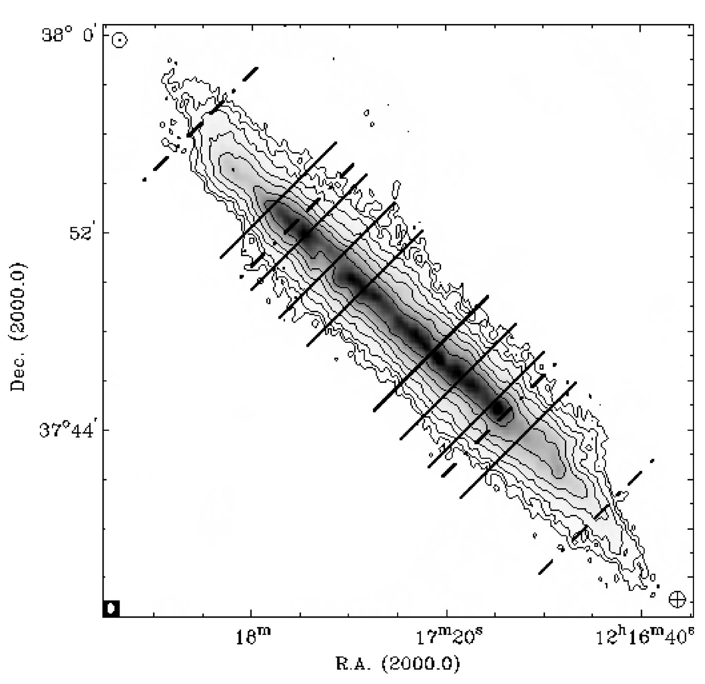

Contours: $4x2^n$ mJy bm^{-1} km s^{-1}

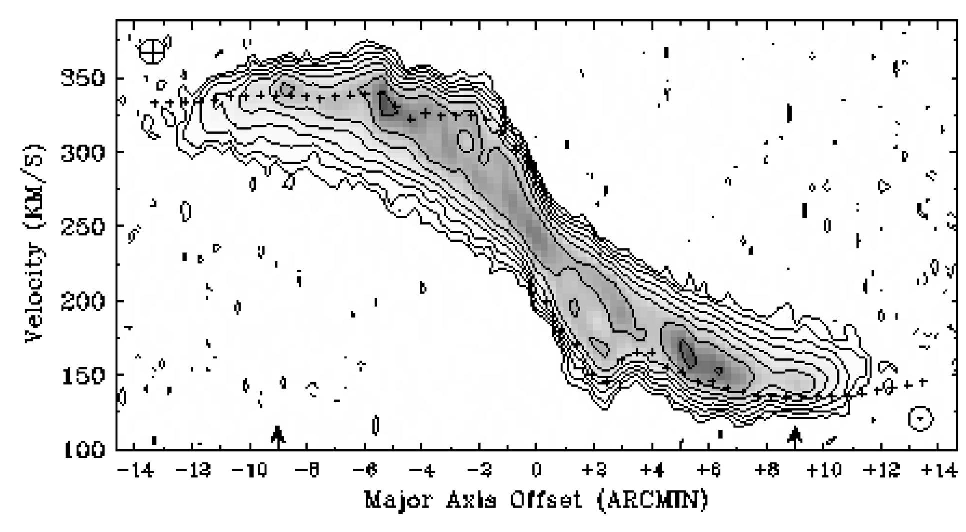

Contours: $0.18x2^n$ mJy bm^{-1}

Figure 2. (above) A major axis pv (lv) diagram with the rotation curve for each half shown in black squares.

The Modeling Process

Model cubes created using the Gronigen Image Processing System (GIPSY) are divided into concentric rings where the column density, rotational velocity, scale height, velocity dispersion, inclination, and position angle for each are specified. A lag may also be added. Due to asymmetries, the approaching and receding halves of NGC 4244 are modeled separately.

Models considered are, in approximate order of complexity:

- One vertical component (1C)
- Warp (W) along the line of sight (LOS)
- Flare (F)
- LOS warp with a flare (WF)
- Two vertical components (halo) (2C)
- Two vertical components (halo) with a LOS warp (2CW)

An "L" is added to the abbreviation if a lag is present.

In all of the models, velocity dispersion (12 decreasing to 10 km s^{-1}), systemic velocity (244 km s^{-1}), kinematic center and the run of the position angle are kept constant. All final models have the same column density profiles and rotation curves.

The minor axis position-velocity (bv) diagrams in Figures 3 and 4 illustrate a number of the most representative features we endeavor to match. Naturally, it is impossible to display all relevant figures at this time although a variety of plots are used. In the end, an acceptable model is one that fits *all* of these plots well.

The Optimal Model for NGC 4244

Based on all plots available during the modeling process, the one component warp model with a lag (WL) is favored. This may be surprising given the plots supplied, as the 2CWL model also appears to fit the bv diagrams well. However, it is clear from the vertical profile (not shown) that there is no motivation for a second component.

The WL and WFL models are nearly indistinguishable. A flare possibly exists in NGC 4244 as described in Olling (1996), but is dominated by the LOS warp, which we find to be the primary source of apparent vertical extent.

Properties of the Lag

The improvement due to the lag is present in all models. This attests to its robustness in that, regardless of the optimal model, there are features which cannot be re-created without it.

For the WL model, the lag is -9+/-2 km s^{-1} kpc^{-1}.

Additionally, the lag in this model displays radial variation, as shown in Figure 5. (approaching half not shown) These diagrams indicate a shallowing of the lag, noticeable around 7' (9 kpc).

Figure 5. 30x30" resolution bv plots showing the radial variation in the lag in the receding half. Data contours are shown in black and model contours in white. Note the extent of each on the terminal as well as the high-z emission on the systemic side. The convention for symbols is the same as that initiated in Figure 4.

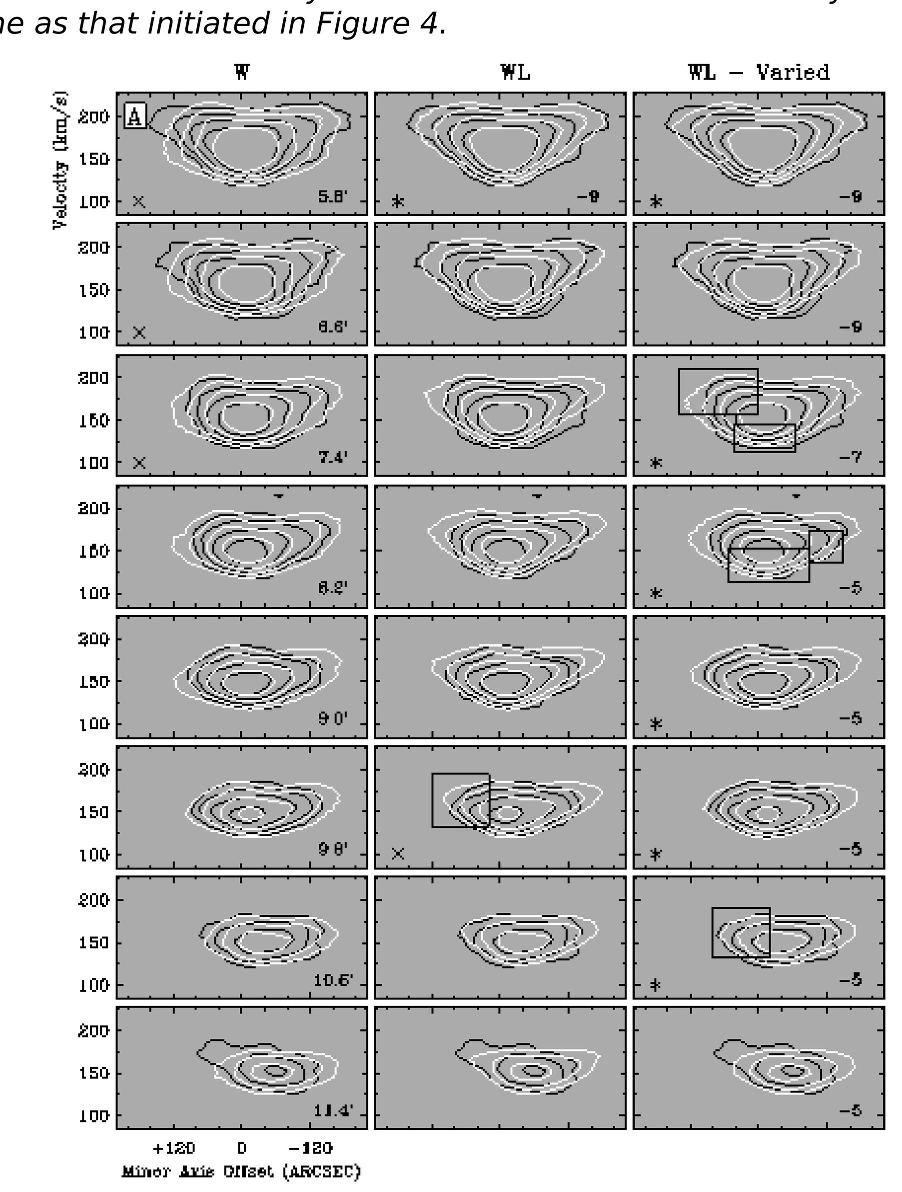

Contours: 0.24x3ⁿ mJy/beam

References

Heald, G., et al. 2011, A&A, 526, 118
Heald, G. H., Rand, R. J., Benjamin, R. A., & Bershady, M. A. 2007, ApJ, 663, 933
Hoopes, C. G., Walterbos, R. A. M., & Rand, R. J. 1999, ApJ, 522, 699
Howk, J. C., & Savage, B. D. 1999, AJ, 117, 2077
Olling, R. P. 199, AJ, 112, 457
Rossa, J., & Dettmar, R. 2003, A&A, 406, 493
Tullmann, R., Breitschwerdt, D., Rossa, J., Pietsch, W., & Dettmar, R. 2006a, A&A, 457, 779

UNM ASTRON UNIVERSITEIT GENT

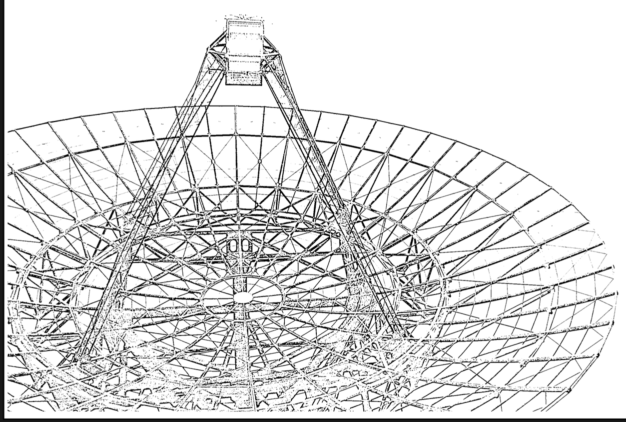

The WSRT HALOGAS Survey: HI Observations and Models of NGC 4565

Laura K. Zschaechner, Richard J. Rand, George H. Heald, and the HALOGAS Team

Introduction

For a brief explanation concerning the motivation for kinematic modeling of extended HI, refer to the previous slide.

NGC 4565 is on the somewhat high end of the HALOGAS sample in terms of SFR (2.7 $M_{\odot}\ yr^{-1}$), and a high inclination (87.5°+/-0.3°), making it useful in determining trends concerning SFR and the existence of extra-planar HI and the magnitudes of lags.

Observations and Data

Details concerning the observations may be found on the HALOGAS website: http://www.astron.nl/halogas/

For NGC 4244, We use a 24.3x11.5" cube with a position angle of -4.69°. Lower resolution cubes will also be examined for fainter emission. The velocity resolution of each cube is 4.12 km/s.

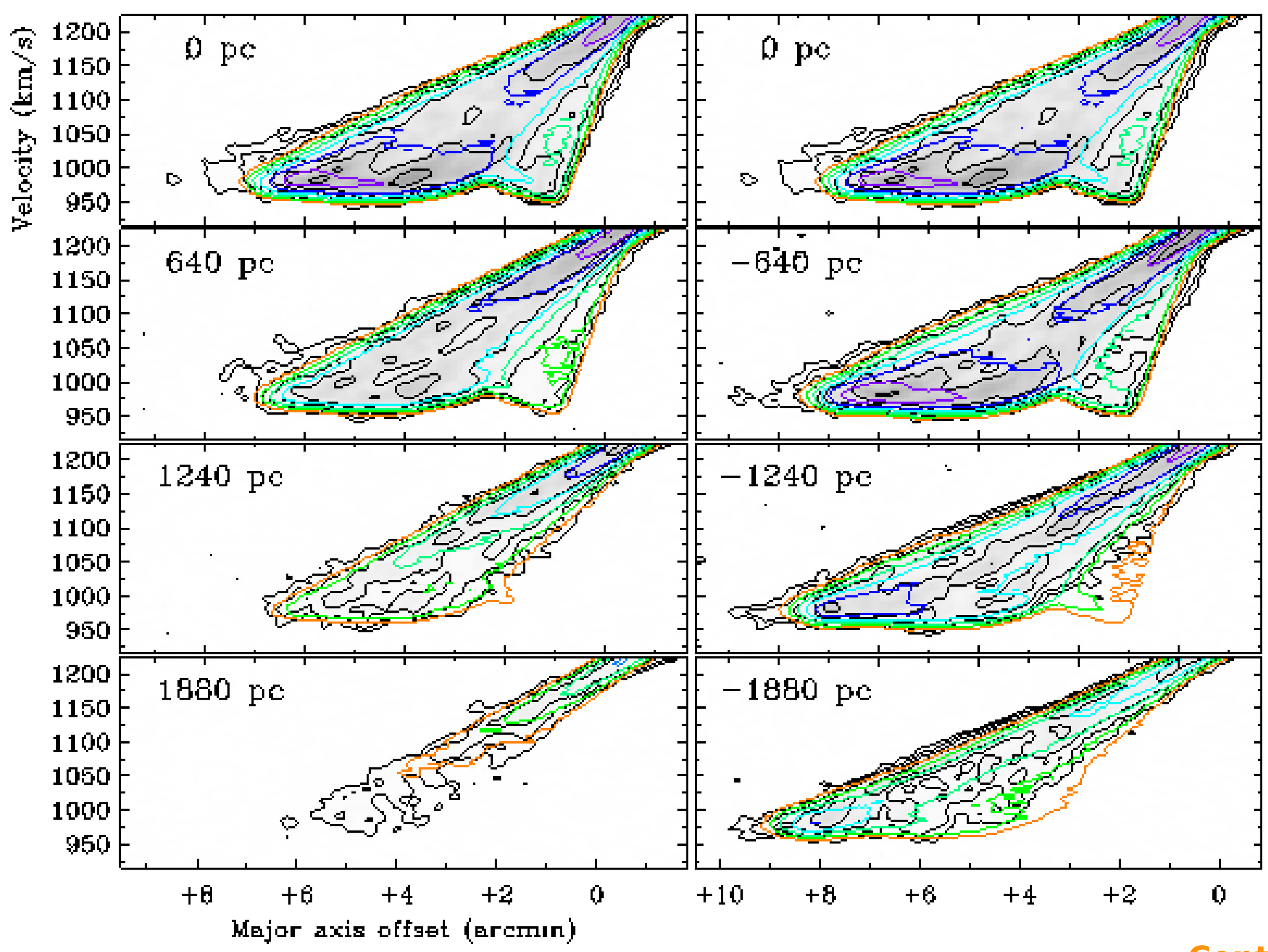

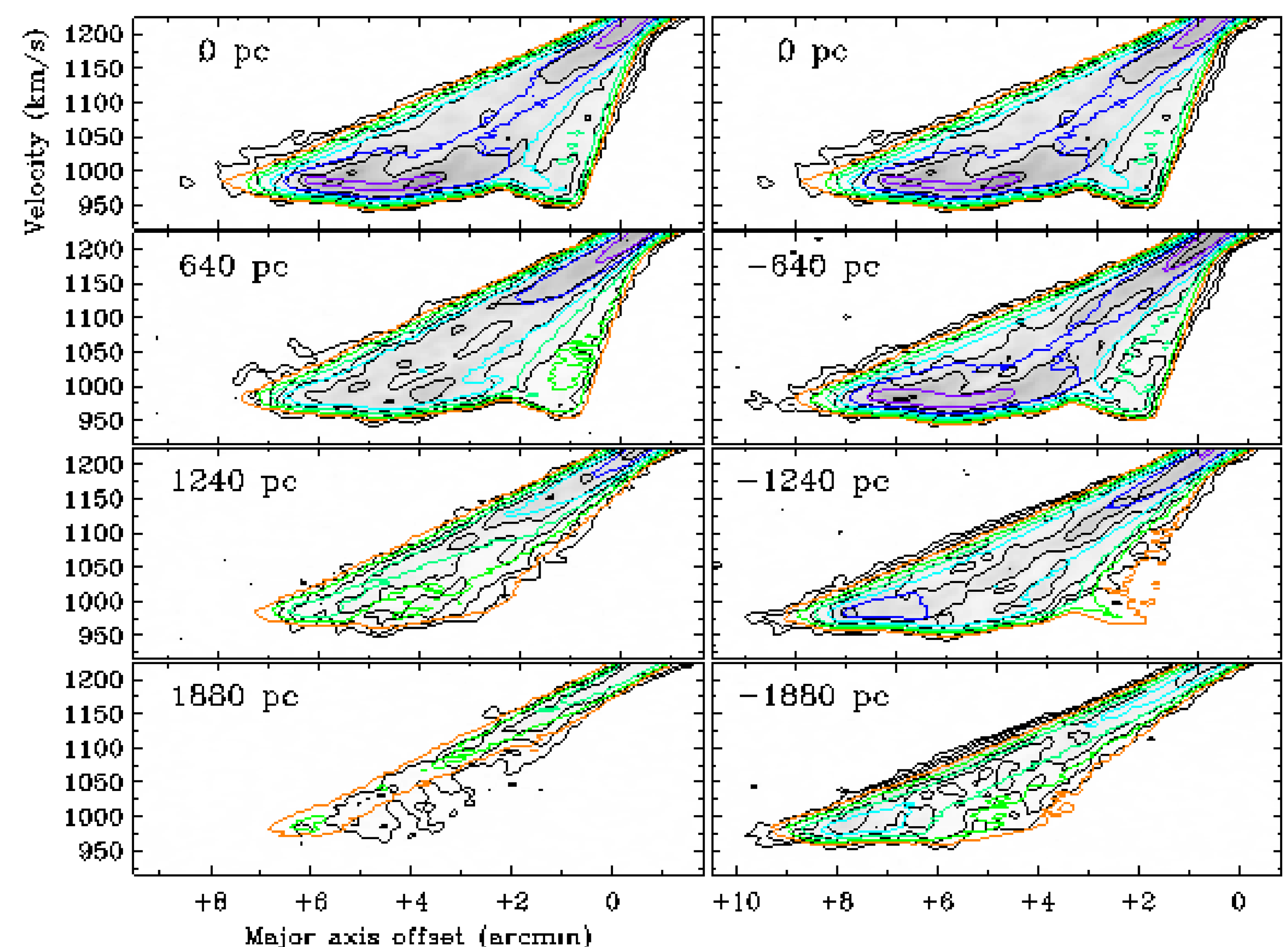

Contours: 0.92x2ⁿ mJy/beam

Figure 1. lv diagrams showing the 1-component model on the approaching half. Data are shown in black contours and grayscale, and model contours in color. Note the spur near the right-hand side of the panel corresponding to -1240 pc, as well as the extent of the model emission compared to the data in the panel corresponding to 1880 pc.

Figure 2. Analogous lv diagrams showing the flaring model. The spur seen in the model is reduced at -1240 pc, and the extent of the model emission more closely matches that of the data at 1880 pc.

The Models

A description of the modeling process may be found on the previous slide.

In all of the models, velocity dispersion (10 km s^{-1}), systemic velocity (1228 km s^{-1}), kinematic center and the run of the position angle are kept constant. All models have the same column density profiles and rotation curves.

Major axis pv diagrams showing 1-component and 1-component flaring models are shown in figures 1 and 2 respectively. Notable improvements from the flare, which is currently the best fit model to the lv diagrams, are:

- The extent of each model to outer radii
- The "spur" best seen in panels corresponding to -1240 pc
- The extent of emission in panels corresponding to 1880 pc.

Remaining Work

The current models will be refined not only by eye, but via a semi-automated tilting ring fitting software, TiRiFiC. (See G. Józsa, also attending this conference for details concerning TiRiFiC itself.) TiRiFiC will allow for a chi-square fit to the data.

Additionally, features such as the high-z HI emission in the NE quadrant will be examined as will be the companion galaxy.

Figure 3.
Zeroth-Moment map of NGC 4565 and two other galaxies, NGC 4562 (SW corner) and IC 3571 (NE corner). HI data indicate that NGC 4565 and IC 3571 are interacting.

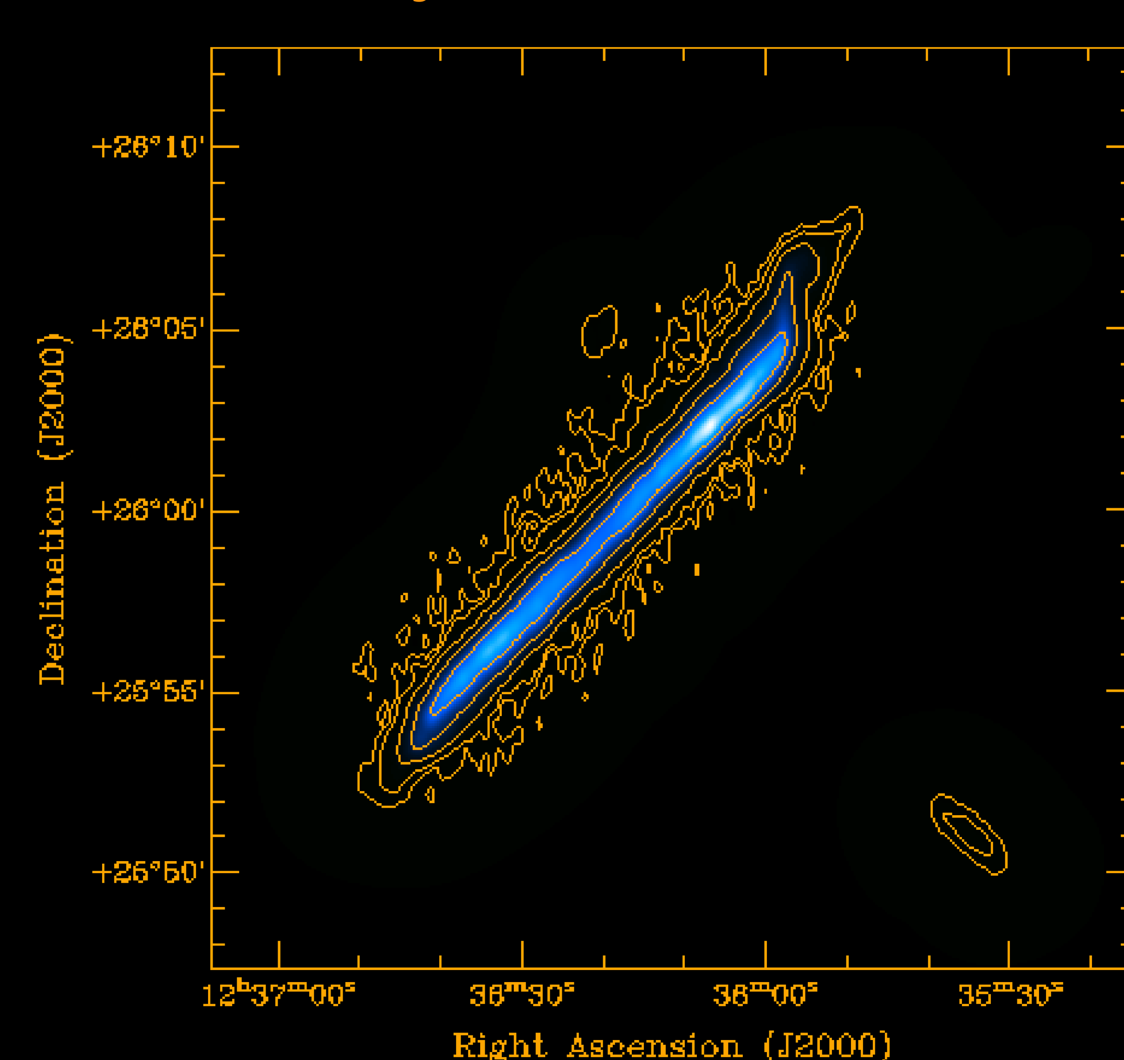

Contours: 2×2^n mJy bm^{-1} km s^{-1}

Current Status of Models

Although the modeling process is at an early stage, the following is becoming apparent:

- There exists a strong warp component across the line of sight.
  - If a line of sight warp component exists, it is comparatively small.
- The addition of a flaring layer appears to improve several features in the lv diagrams.
- The inclination is 87.5°+/-0.3°.
- There is no evidence for a lag.

References

Heald, G., et al. 2011, A&A, 526, 118

Józsa, G. I. G et al. 2007, A&A, 468 731